Molecular Therapy
Nucleic Acids
Original Article

Activating the Cpx response induces tolerance to antisense PNA delivered by an arginine-rich peptide in *Escherichia coli*

Jakob Frimodt-Møller,[1] Andreas Koulouktsis,[1] Godefroid Charbon,[1] Marit Otterlei,[2] Peter E. Nielsen,[3] and Anders Løbner-Olesen[1]

[1]Department of Biology, Center for Peptide-Based Antibiotics, University of Copenhagen, Ole Maaløes vej 5, 2200 Copenhagen N, Denmark; [2]Department of Clinical and Molecular Medicine, Faculty of Medicine and Health Sciences, NTNU, Norwegian University of Science and Technology, NO-7489 Trondheim, Norway; [3]Department of Cellular and Molecular Medicine, Center for Peptide-Based Antibiotics, The Panum Institute, Faculty of Health and Medical Sciences, University of Copenhagen, Blegdamsvej 3B, 2200 Copenhagen N, Denmark

Cell-penetrating peptides (CPPs) are increasingly used for cellular drug delivery in both pro- and eukaryotic cells, and oligoarginines have attracted special attention. How arginine-rich CPPs translocate across the cell envelope, particularly for prokaryotes, is still unknown. Arginine-rich CPPs efficiently deliver antimicrobial peptide nucleic acid (PNA) to its intracellular mRNA target in bacteria. We show that resistance to PNA conjugated to an arginine-rich CPP in *Escherichia coli* requires multiple genetic modifications and is specific for the CPP part and not to the PNA part. An integral part of the resistance was the constitutively activated Cpx-envelope stress response system (*cpx), which decreased the cytoplasmic membrane potential. This indicates an indirect energy-dependent uptake mechanism for antimicrobials conjugated to arginine-rich CPPs. In agreement, *cpx** mutants showed low-level resistance to aminoglycosides and an arginine-rich CPP conjugated to a peptide targeting the DNA sliding clamp, i.e., similar uptake in *E. coli* for these antimicrobial compounds.**

INTRODUCTION

Antimicrobial resistance is one of the major challenges of the 21st century. Thus, efforts to bring novel antimicrobial compounds, including antimicrobial peptides (AMPs), into clinical use are accelerating. Antisense technology, as a gene-targeted precision drug modality, has recently produced several new drugs in clinical use (e.g., nusinersen, inotersen, valonesorsen, and golodirsen), and agents based on the pseudopeptide DNA mimic peptide nucleic acid (PNA)[1] and phosphorodiamidate morpholino oligomer (PMO)[2] have been proposed as future antibiotics. The hydrophobic nature of cellular membranes makes them impermeable for most proteins, peptides, and oligonucleotides, including PNA and PMO.[2,3] Hence, these require a carrier molecule (e.g., cell-penetrating peptide [CPP]) for efficient translocation into the cytoplasm. CPPs are generally short peptides rich in basic (lysine and arginine) and hydrophobic amino acids. Polyarginine enters the cell more efficiently than other polycationic homopolymers (including polylysine),[4] and arginine-rich CPPs are also the most extensively employed and studied.[5] Nonetheless, it is poorly understood how these translocate into both eukaryotic and prokaryotic cells. In eukaryotes, evidence supports predominantly an energy-dependent endocytotic pathway, although energy-independent direct translocation may also play a role.[6] Very little is known about how CPPs conjugated to PNA/PMO/AMPs penetrate through the lipid membranes of the envelope in prokaryotes, and for CPPs conjugated to PNA (CPP-PNA) only one paper has addressed this topic.[7] Here, PNA conjugated to the lysine-phenylalanine-rich CPP $L((KFF)_3K)$ enters *Escherichia coli* by the non-essential inner membrane transporter SbmA;[7] consequently, SbmA-deficient *E. coli* are highly resistant to PNA delivered by this peptide. On the other hand, PNA conjugated to an arginine-rich CPP, $(R\text{-}Ahx\text{-}R)_4$-Ahx-(βAla) (RXR), enters the cell in an unknown and SbmA-independent manner.[7]

The envelope of Gram-negative bacteria consists of three structurally and chemically diverse layers: (1) the inner/cytoplasmic membrane (consisting of phospholipids); (2) the periplasm containing a thin peptidoglycan layer; and (3) the outer membrane that contains phospholipids in the inner leaflet and phospholipids and lipopolysaccharide (LPS) in the outer leaflet. The role of the Gram-negative envelope is multifaceted, i.e., it is a barrier that prevents toxic molecules, such as antimicrobials, from entering, meanwhile facilitating the entry of molecules vital for growth (by either dedicated transport or diffusion). When faced by antimicrobial agents, bacteria are able to adapt and survive this selective pressure in numerous ways, including (over)

Received 8 January 2021; accepted 16 June 2021;
https://doi.org/10.1016/j.omtn.2021.06.009.

Correspondence: Anders Løbner-Olesen, Department of Biology, Center for Peptide-Based Antibiotics, University of Copenhagen, Ole Maaløes vej 5, 2200 Copenhagen N, Denmark.
E-mail: lobner@bio.ku.dk
Correspondence: Jakob Frimodt-Møller, Department of Biology, Center for Peptide-Based Antibiotics, University of Copenhagen, Ole Maaløes vej 5, 2200 Copenhagen N, Denmark.
E-mail: jakob.frimodtmoller@bio.ku.dk

expression of efflux pumps, drug target modification, modification of the cell envelope, inactivation, or modification of the drug.[8]

E. coli can actively transport compounds across the cytoplasmic membrane using either ATP hydrolysis or the chemical proton gradient (part of the proton motive force [PMF]), which is generated by translocating protons from the cytoplasm into the periplasmic space,[9] via the electron transport chain. The energetics of the cell varies considerably between growth with or without oxygen, with oxidative growth conditions providing the highest energy turnover. For instance, PMF is decreased during anoxic growth conditions.[10] Under aerobic conditions the electron transport chain predominantly contains NADH:ubiquinone oxidoreductase complex I (encoded by the *nuoABCEFGHIJKLMN*-operon; NDH-I) and cytochrome bo_3 ubiquinol oxidase (encoded by the *cyoABCDE* operon; cytochrome bo_3 oxidase).[9] The PMF generated serves as energy storage, which is used to drive, e.g., F_1F_0-ATPase,[11] efflux pumps, and transport of metabolites.[12] The PMF across the cytoplasmic membrane is a combination of the electric potential ($\Delta\Psi$) and the transmembrane proton gradient (ΔpH: internal pH − external pH). $\Delta\Psi$ is always negative inside growing neutrophils with a cytosolic pH environment between 6.5 and 7.5 such as *E. coli*, and $\Delta\Psi$ decreases as ΔpH increases,[10] i.e., bacteria may regulate $\Delta\Psi$ and/or ΔpH in order to control PMF.

The Cpx, Bae, Psp, Rcs, and σ^E signaling systems detect alterations to the bacterial envelope. These pathways are involved in the biogenesis, maintenance, and repair of the bacterial envelope and thus contribute to cell surface integrity.[13] One of the most well-studied extracytoplasmic stress response systems is the CpxA/R two-component signal transduction system, which when activated controls a number of genes including respiratory enzymes that are downregulated.[14] Like many other histidine kinases, CpxA is localized to the cytoplasmic membrane through two transmembrane helices and contains both periplasmic and cytoplasmic domains.[15] The cytoplasmic response regulator, *cpxR*, is predicted to encode an OmpR-like transcriptional activator.[15] CpxR consists of an N-terminal receiver domain (phospho-acceptor domain) and a C-terminal DNA-binding domain.[16] Under non-stress conditions the auxiliary regulator CpxP inhibits the Cpx response by a predicted direct interaction with the periplasmic domain of CpxA.[17] Under Cpx-inducing conditions, CpxP is degraded by the periplasmic protease and chaperone DegP.[18] The CpxP-relieved CpxA autophosphorylates on a conserved histidine residue (His-248), using ATP as its phosphoryl donor.[19] Subsequently, phosphorylated CpxA donates its phosphoryl group to the conserved aspartate residue (Asp-51) in the N-terminal receiver domain of CpxR. Phosphorylated CpxR binds to DNA and acts as a transcriptional regulator.[19] In addition, CpxA dephosphorylates CpxR-P, which ensures that CpxR remains inactive in the absence of an activating signal.[20] The outer membrane lipoprotein NlpE that senses surface adhesion acts as a "sentry protein" against envelope stress and activates the Cpx-response system through an undefined interaction with CpxA.[20] *cpxP* is the most highly inducible gene of the Cpx regulon, and expression of this is used as a representative of an activated Cpx response.[17]

Here we show that a constitutive Cpx response, resulting in a decreased $\Delta\Psi$ across the cytoplasmic membrane, reduces drug delivery by arginine-rich CPPs to their intracellular targets. The decreased $\Delta\Psi$ also confers cross-resistance to aminoglycosides, indicating a similar uptake mechanism for the two classes of compounds.

RESULTS

To understand bacterial uptake and resistance to PNA conjugated to an arginine-rich CPP, we studied the widely used RXR[7] (Table 1). Unless stated otherwise, the PNA part always targets translation of the *acpP* mRNA, encoding the acyl carrier protein, which is essential for fatty acid synthesis.[7] RXR-PNA had a minimum inhibitory concentration (MIC) of 0.5 μM toward *E. coli*. Because PNA containing two mismatches (PNA_{mm}) showed no inhibition (up to 16 μM) of bacterial growth, the antibacterial activity of RXR-PNA is specific to the PNA part, whereas the delivery peptide part alone did not confer any antimicrobial effect but only promotes cellular uptake of the conjugated PNA (Table 1). A previous study failed to identify single-gene deletion mutants of *E. coli* that promoted tolerance to RXR-PNA.[7] We therefore used adaptive laboratory evolution (ALE; see Materials and methods) to generate RXR-PNA-resistant mutants. Here, we grew wild-type cells in successively increasing concentrations of RXR-PNA, selecting for mutation(s) that enabled survival at high concentration. The ALE experiments were done in two independent linages (i.e., lineage one and two) and was terminated after 20 successive passages, where clones appeared with a 16-fold increase in MIC (from 0.5 μM to 8 μM) (Table 1), which we define as RXR-PNA resistance.

Five individual clones from each lineage at day 20 (ten clones in total) were isolated and sequenced (Table 2; Tables S1 and S2). From the ten resistant clones, we identified three unique genotypes, which were annotated Evo-1, Evo-2, and Evo-3. Evo-1 and 2 were present in two and three clones of lineage one, respectively, whereas the Evo-3 genotype was found in all five sequenced clones of lineage two. None of the mutations identified in the ALE experiment resulted from adaptation to the growth medium, as they were not present in wild-type cells adapted to the same growth medium without RXR-PNA (Table S3).

All sequenced clones shared an IS5 insertion in the *gltF-yhcA* intergenic region, IS1 insertions in *waaB* and *waaO,* and the $rpsL_{I82N}$ mutation (Table 2). *gltF* belongs to the *gltBDF*-operon, where *gltB* and *gltD* encode the large and small subunit of glutamate synthase,[23] respectively. The function of GltF and the hypothetical protein YhcA is unknown. The *waa*-operon encodes enzymes for assembly of the major core oligosaccharide of LPS.[24] *rpsL* is the only mutated gene that is essential. The product of *rpsL* is the S12 protein, a component of the 30S subunit of the ribosome, where it plays a role in translational accuracy.[25] The role of $rpsL_{I82N}$ in tolerance to RXR-PNA will not be pursued here.

Table 1. Minimum inhibitory concentration to peptide-PNA (in μM)

				RXR-PNA resistant strains		
Compound[a]	CPP	Target gene/protein	Wild type	Evo-1	Evo-2	Evo-3
RXR-PNA[7]	arginine-rich RXR[a]	*acpP*[d]	0.5	8	8	8
$RXR\text{-}PNA_{mm}$[7]		*acpP* mismatch[e]	>16	>16	>16	>16
$RXR\text{-}PNA_{ftsZ}$[7]		*ftsZ*[f]	0.5	8	8	8
$RXR\text{-}PNA_{ftsZ\_mm}$[7]		*ftsZ* mismatch[g]	>16	> 6	>16	>16
R11-APIM[21]	arginine-rich R11[b]	β-clamp (*dnaN*)[h]	1	N/A	N/A	N/A
KFF-PNA[7]	lysine-phenylalanine KFF[c]	*acpP*[d]	0.25	0.25	0.25	0.25
$KFF\text{-}PNA_{mm}$[7]		*acpP* mismatch[f]	>16	>16	>16	>16

MIC determinations for peptide-PNA are in μM. MICs were determined with broth dilutions (see Materials and methods) at 37°C (no shaking).
[a]Arginine-rich RXR: H-(R-Ahx-R)$_4$-Ahx-(βAla). For the CPP part amino acids are shown in uppercase letters. Ahx, 6-aminohexanoic acid.
[b]Arginine-rich R11: RRRRRRRRRRR.
[c]Lysine-rich KFF: H-(KFF)$_3$K-eg1.
[d]*acpP* target sequence (5′–3′): H-ctcatactct-NH_2.
[e]*acpP* mismatch sequence (the two mismatches are underlined, 5′–3′): H-ctcttacact-NH_2.
[f]*ftsZ* target sequence (5′–3′): H-ttcaaacatagt-NH_2.
[g]*ftsZ* mismatch sequence (the two mismatches are underlined, 5′–3′): H-ttctaacaaagt-NH_2.
[h]Ac-MD-RWLVK-GILQWRKI (RWLVK*).

Resistance to RXR-PNA is toward the arginine-rich CPP part and not the PNA part

The Evo-1, Evo-2, and Evo-3 mutants were also resistant to RXR conjugated to a PNA targeting the essential division protein *ftsZ*; however, they remained sensitive to a PNA conjugated to the lysine-phenylalanine-rich CPP, *L*((KFF)$_3$K), KFF-PNA targeting *acpP* (Table 1). Thus, the RXR-PNA resistance of Evo-1, Evo-2, and Evo-3 followed the CPP delivery peptide and not the PNA part, supporting the notion of a different uptake mechanism for the RXR peptide compared to KFF, which is transported across the cytoplasmic membrane by SbmA.[7]

No apparent role for GltF or YhcA in tolerance to RXR-PNA

To understand the effect of the conserved IS5 insertion in the *gltF-yhcA* intergenic region on tolerance to RXR-PNA, *gltF* and *yhcA* were individually deleted in the wild-type cell, resulting in Δ*gltF* and Δ*yhcA*, respectively. However, neither *gltF* nor *yhcA* deficiency had any effect on susceptibility to RXR-PNA compared to wild type (Figure 1A). Additionally, overproduction of *gltF* or *yhcA,* in the wild-type cells, led to no changes in MIC toward RXR-PNA (Figure 1A). Hence, the importance of the IS5 insertion in the *gltF-yhcA* intergenic region to RXR-PNA tolerance is presently unknown.

The outer membrane is not the main barrier for RXR-PNA

During uptake the arginine-rich delivery peptide RXR must first interact with the outer membrane, which is the main barrier for some compounds, including cationic (antimicrobial) peptides.[26] Evo-1, Evo-2, and Evo-3 mutants all had IS1 insertions in *waaB* and *waaO*, expected to result in LPS with a deficient outer core. We therefore deleted *waaBO* in the wild-type cells but observed no changes in susceptibility to RXR-PNA (Figure 1A). Hence, the outer membrane provides a limited or no barrier for RXR-PNA. Thus, attention was turned to the role of the cytoplasmic membrane as a barrier for arginine-rich CPPs. Here, the mutation in *cpxR* was identified in all clones of lineage two (Evo-3) and stood out because of its involvement in extracytoplasmic stress response through the cytoplasmic membrane sensor, CpxA, and its regulator, CpxR.[27]

An activated Cpx response leads to tolerance to antimicrobials delivered by arginine-rich CPPs

Loss of the Cpx response, by deletion of *cpxA* or *cpxR*, in otherwise wild-type cells had no effect on RXR-PNA sensitivity (Figure 1B), while increased levels of CpxR (i.e., activation of the Cpx response) led to a small but reproducible decrease in susceptibility (Figure 1B). We proceeded to introduce the $cpxR_{L20Q}$ mutation identified in the ALE experiment (Table 2) into wild-type cells and included a $cpxA_{\Delta 16\text{-}17}$ mutant that was isolated in a different project. In $CpxR_{L20Q}$, leucine is replaced by glutamine at position 20, which is part of a highly conserved hydrophobic core in the N-terminal receiver domain shared by OmpR family proteins.[16] In $CpxA_{\Delta 16\text{-}17}$ threonine at position 16 and leucine at position 17, located in the first CpxA transmembrane domain, are missing. Introduction of both $cpxR_{L20Q}$ and $cpxA_{\Delta 16\text{-}17}$ mutations in wild-type cells resulted in an increased MIC to RXR-PNA from 0.5 μM to 4 μM, relative to wild-type cells (Figure 1B). However, the $cpxR_{L20Q}$ and $cpxA_{\Delta 16\text{-}17}$ mutants did not reach the RXR-PNA resistance level of Evo-1 to 3. Because of the low-level resistance to RXR-PNA, the $cpxR_{L20Q}$ and $cpxA_{\Delta 16\text{-}17}$ mutants were tested against an oligoarginine conjugate to a AMP targeting the DNA sliding clamp (DnaB; β-clamp) (RWLVK-GILQWRKI-RRRRRRRRRRR; R11-APIM). R11-APIM was shown to inhibit bacterial growth at micromolar concentrations both *in vitro* and *in vivo*[21] (Table 1). Here, $cpxR_{L20Q}$ and $cpxA_{\Delta 16\text{-}17}$ had a decrease in susceptibility to R11-APIM analogous to the observation for RXR-PNA, although the magnitude was smaller (Figure 1C);

Table 2. RXR-PNA resistant genotypes

					Evolved toward RXR-PNA		
				Lineage[c]	#1		#2
Mutation type[a]				No.[d]	2/5	3/5	5/5
IS	DEL	SNP	Region/gene[b]	Strain	Evo-1	Evo-2	Evo-3
IS1			IG: *chbB–osmE*		x	x	
IS5			IG: *gltF–yhcA*		x	x	x
IS1			*rapA*		x	x	
IS1			*waaB*		x	x	x
IS1			*waaO*		x	x	x
		x	$yfaP_{V55G}$		x		
		x	$rpsL_{I82N}$		x	x	x
		x	$bdcA_{A53T}$		x		
		x	$cpxR_{L20Q}$				x
	x		*Δrac*			x	

Mutational profile of RXR-PNA^{R} clones. See Table S1 for mutation details and Table S2 for function of the mutated genes.
[a]Mutation type; IS, IS insertion; DEL, deletion; SNP, single-nucleotide polymorphism.
[b]Mutated genomic region; IG, intergenic region between two genes; Δ*rac*, excerted *rac* prophage.[22]
[c]Lineage from which the evolved clones were isolated within the ALE experiment with RXR-PNA.
[d]Number of the evolved clone within the lineage.

tolerance to R11-APIM was only 2-fold increased compared to 8-fold for the RXR-PNA.

To assess whether the $cpxA_{\Delta 16\text{-}17}$ and $cpxR_{L20Q}$ mutations were dependent on a functional Cpx system for low-level resistance to RXR-PNA, *cpxA* was deleted in the $cpxR_{L20Q}$ strain and *cpxR* was deleted in the $cpxA_{\Delta 16\text{-}17}$ strain. In either case, the MIC for RXR-PNA was reduced to wild-type level (Figure 1B). Thus, the substitution to glutamine in position 20 in CpxR does not make it constitutively active by mimicking phosphorylation of the conserved Asp-51, and $CpxR_{L20Q}$ still relies on a functional CpxA to be activated. Overproduction of wild-type CpxR or CpxA in the $cpxR_{L20Q}$ or $cpxA_{\Delta 16\text{-}17}$ mutants, respectively, also restored RXR-PNA susceptibility to wild-type level (Figure 1B). Together, this indicates that the specific $cpxR_{L20Q}$ or $cpxA_{\Delta 16\text{-}17}$ mutation mediates low-level resistance to RXR-PNA but relies on a functional Cpx system.

The Cpx response is activated in $cpxA_{\Delta 16\text{-}17}$ and $cpxR_{L20Q}$ and is the only extracytoplasmic stress response conferring tolerance to RXR-PNA

We used *cpxP* transcription as a readout for activation of the *cpx* response.[28] $cpxR_{L20Q}$, $cpxA_{\Delta 16\text{-}17}$, and Evo-3 all had significant increased expression of *cpxP* compared to wild-type (Figure 2A), albeit not to the level achieved by overproduction of NlpE (full activation of the Cpx response; Figure 2A). This confirmed that the Cpx response was indeed activated by the $cpxR_{L20Q}$ and $cpxA_{\Delta 16\text{-}17}$ mutations. Accordingly, NlpE overproduction also provided tolerance to RXR-PNA to the same level (compare Figure 1B to Figure 2B). Both $cpxR_{L20Q}$ and $cpxA_{\Delta 16\text{-}17}$ are therefore gain-of-function mutations leading to a constitutively active Cpx response, which previously have been denoted *cpx**.[19,20]

The Cpx response is only one of five extracytoplasmic stress response systems known to maintain cell envelope integrity during stress. Whereas the Cpx response can be activated by overproducing *nlpE,* the four other extracytoplasmic stress responses can be individually activated by overproduction of BaeR for the Bae pathway, RcsB for the Rcs pathway, PspF for the Psp pathway, and RpoE for the σ^E pathway.[13] Expression of the cloned genes was induced by addition of isopropyl β-D-1-thiogalactopyranoside (IPTG). Because overexpression of PspF[13] and RpoE[29] is toxic, we determined the minimal IPTG concentration that resulted in activation of the extracytoplasmic stress responses with minimal cell toxicity. RcsB and BaeR synthesis was induced with 0.1 mM IPTG, whereas PspF and RpoE synthesis was induced with 0.01 mM IPTG (Figure S1). Overexpression of RpoE appeared particularly toxic to the cell (Figure S1), and we cannot exclude that suppressor mutations had formed; nor can we exclude plasmid loss and/or rearrangement. Activation of neither the Bae, Psp, Rcs, nor the σ^E responses led to an altered susceptibility to RXR-PNA compared to the wild type (Figure 2B), supporting that this is specific to the activated Cpx response. The presence of RXR-PNA at sub-MIC concentrations (0.5× MIC) did not activate the Cpx response in wild-type cells (no increased *cpxP* expression; Figure 2A). Hence, although an activated Cpx response confers RXR-PNA tolerance, low-level RXR-PNA treatment in itself does not trigger the extracytoplasmic stress response.

Cpx-dependent downregulation of respiratory operons leads to tolerance to antimicrobials delivered by arginine-rich CPPs and to aminoglycosides

We determined *nuoA* (to evaluate expression of the *nuoABCEFGHIJKLMN* operon) and *cyoA* (to evaluate expression of the *cyoABCDE* operon) transcription by qRT-PCR. Both operons were significantly downregulated in cells with a constitutively activated Cpx response: NlpE overproduction: $cpxR_{L20Q}$, $cpxA_{\Delta 16\text{-}17}$, and Evo-3 cells (Figure 3A). In agreement, an activated Cpx response has been reported to downregulate aerobic respiratory operons.[14] When the entire *nuoABCEFGHIJKLMN* or *cyoABCDE* operon was individually deleted in wild-type cells, the resultant Δ*nuo* and Δ*cyo* strains confered low-level resistance to RXR-PNA, R11-APIM (Figure 3B), as well as the aminoglycosides gentamicin, amikacin, and kanamycin (Figure 3C). This shows that low-level resistance to both arginine-rich CPPs and aminoglycosides in *cpx** cells results from reducing oxidative phosphorylation through downregulation of NDH-I and cytochrome bo_3 oxidase.

The cytoplasmic membrane potential correlates with RXR-PNA, R11-APIM, and aminoglycoside activity

We determined the cytoplasmic membrane potential ($\Delta\Psi$) at the intracellular pH 7.6 based on the distribution of the lipophilic tetraphenylphosphonium ion (TPP^+), using a TPP^+-selective electrode.[30] At this pH value, ΔpH is zero and the PMF is equal to $\Delta\Psi$. Wild-type

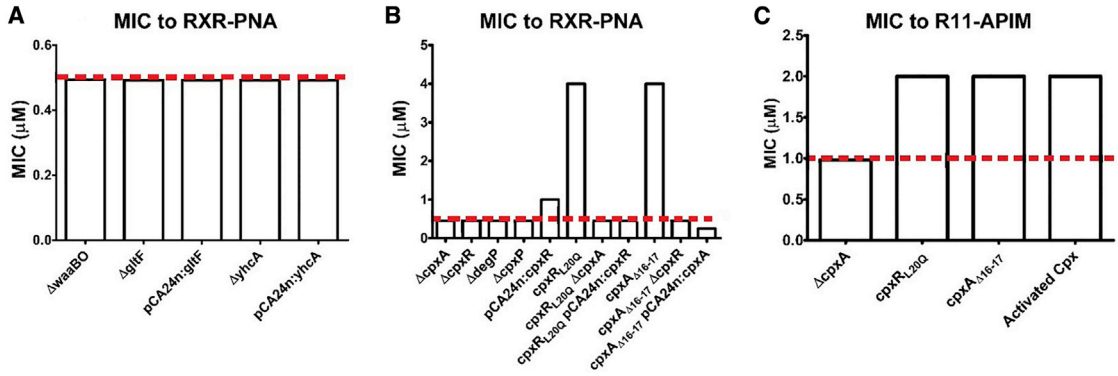

Figure 1. *cpxR*$_{L20Q}$ and *cpxA*$_{Δ16-17}$ confer RXR-PNA tolerance

(A–C) MIC determinations for RXR-PNA/R11-APIM for wild type and mutants in μM. MICs were determined with broth dilutions (see Materials and methods) at 37°C (no shaking). Peptide-PNA sequences are listed in Table 1. pCA24n-based plasmids were induced with 0.1 mM IPTG.

cells had a ΔΨ of approximately −140 mV, in accordance with previous observations[31] (Figure 4A). The ΔΨ was significantly reduced by the *cpxR*$_{L20Q}$ as well as the *cpxA*$_{Δ16-17}$ mutation (Figure 4A). Δ*cyo* and Δ*nuo* cells also had a significantly decreased ΔΨ compared to wild type, with values comparable to *cpxR*$_{L20Q}$ and *cpxA*$_{Δ16-17}$ (Figure 4A). Thus, it is conceivable that the decreased ΔΨ of *cpxR*$_{L20Q}$ and *cpxA*$_{Δ16-17}$ cells results from downregulation of the respiratory operons.

When wild-type cells are grown anaerobically or in acidic medium (pH 6), the ΔΨ part of the PMF is decreased[10] (Figure 4B). This is also the case when cells are treated with carbonyl cyanide *m*-chlorophenyl hydrazine (CCCP) (Figure 4C), which uncouples the proton gradient because of its ability to act as a ionophore.[32] All treatments that reduced ΔΨ resulted in decreased sensitivity to RXR-PNA, R11-APIM, and aminoglycosides (Figures 4B and 4C). On the other hand, when the ΔΨ part of the PMF is increased by growing in an alkaline medium (pH 8.0)[10] (Figure 4D), by deletion of the F_1F_0-ATPase[33] (Figure 4D), or if growth is supplemented with alanine[34] (Figure 4E), sensitivity to RXR-PNA, R11-APIM, and aminoglycosides was increased. Moreover, sensitivity to KFF-PNA was not affected by changes of the ΔΨ across the cytoplasmic membrane (Figures 4B and 4D), in agreement with a different uptake mechanism for the KFF peptide.

Neither *cpxR*$_{L20Q}$ nor the *cpxA*$_{Δ16-17}$ mutations conferred resistance to cationic antimicrobial peptides

Cationic AMPs represent the biggest class of AMPs, and the majority of these are amphipathic. Here, Cap11, Cap18, cecropin P1, apidaecin 1B, indolicidin, protamine, and the most well-known polypeptide antibiotic, colistin, were tested against wild type, *cpxR*$_{L20Q}$, *cpxA*$_{Δ16-17}$, and Evo-3 (Table 3). Colistin,[35] Cap11,[26] Cap18,[26,36] protamine,[37] and cecropin P1[38] are believed to target the cell envelope (disruption of bilayers), whereas indolicidin (disruption of bilayers and DNA synthesis)[39] and apidaecin 1B (ribosomes)[40] have intracellular targets. An activated Cpx response and a decrease in ΔΨ did not confer tolerance to any of the tested AMPs (Table 3). Interestingly, the evolved strain Evo-3 was more susceptible to cecropin P1, Cap11, Cap18, and colistin than wild type (Table 3), most likely due to by the presence of IS1 insertions in *waaB* and *waaO* in the Evo-3 (Table 2).[26] Accordingly, Δ*waaBO* cells also became more susceptible to cecropin P1, Cap11, Cap18, and colistin.

RXR-PNA resistance is associated with a fitness cost

The doubling times of *cpxR*$_{L20Q}$ and *cpxA*$_{Δ16-17}$ mutants were 28 min and 27 min, respectively, when grown aerobically in Müller-Hinton I Broth (MHBI) at 37°C, somewhat slower than that of wild-type cells (25 min). Of interest, the evolved mutant, Evo-3 (58 min), which conferred the highest resistance to RXR-PNA, grew more than twice as slowly as both the wild type and the *cpxR*$_{L20Q}$ and *cpxA*$_{Δ16-17}$ mutants. This shows that resistance to RXR-PNA came with a high fitness cost.

DISCUSSION

We have isolated and characterized mutants resistant toward (R-Ahx-R)$_4$-Ahx-(βAla)-PNA. Obtaining these proved difficult, most likely because it required additive mutations, and came with a high fitness cost, showing promise for the possible future medical use of CPP-PNA. The increased resistance to RXR-PNA was in part due to a constitutively active Cpx response, which mediates a decrease in ΔΨ across the cytoplasmic membrane. This phenotype conferred cross-resistance to aminoglycosides and R11-APIM, indicating a similar uptake between the antibacterial compounds. These observations highlight the importance of extracytoplasmic stress response in modulating the cytoplasmic membrane to avoid growth cessation by AMPs with intracellular targets.

Reduced arginine-rich CPP uptake arises in multiple steps

The finding that three RXR-PNA-resistant mutants arose across the two lineages in the ALE experiment indicates either multiple ways to confer resistance or that they all confer a similar resistance phenotype. Nonetheless, resistance to RXR-PNA is complex, requiring multiple mutations in independent loci (Table 2). This is in stark contrast to the straightforward route to restrict KFF translocation, by a loss-of-function mutation in the *E. coli sbmA* gene,[7] which inhibits uptake across the cytoplasmic membrane. We show that the *cpx** phenotype

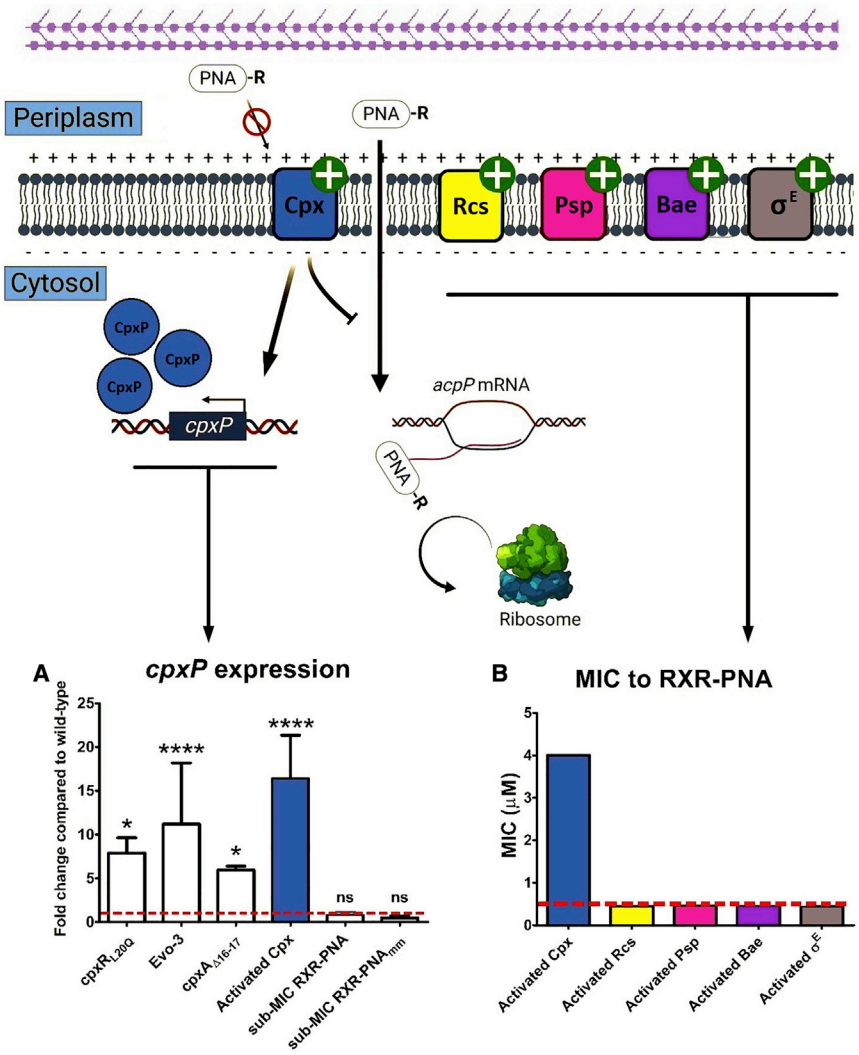

Figure 2. *cpxR*$_{L20Q}$ and *cpxA*$_{Δ16-17}$ activate the Cpx response

A schematic model of the Cpx, Rcs, Psp, Bae, and σ^E stress response to CPP_{RXR}-PNA in the cytoplasmic membrane. Here, RXR-PNA does not activate the Cpx response; however, an activated Cpx response is the only of the five tested extracytoplasmic stress responses that diminish RXR-PNA activity. The green plus sign indicates a constitutive active extracytoplasmic stress response where an activated Cpx response confers resistance to RXR-PNA and R11-APIM. (A) *cpxP* expression determined by qRT-PCR(see Materials and methods). All values are indicated as fold change relative to wild type (dashed line). Experiments were performed in triplicate. Significant differences are identified (*$p < 0.05$, **$p < 0.01$, ****$p < 0.0001$) as determined by Bonferroni's multiple-comparison post-test. (B) MIC determinations for activated extracytoplasmic stress response systems in μM (see text for details). The five extracytoplasmic stress responses were individually activated by overproduction of *nlpE* for the Cpx pathway, *baeR* for the Bae pathway, *rcsB* for the Rcs pathway, *pspF* for the Psp pathway, and *rpoE* for the σ^E pathway.[13] A dashed line indicates the wild-type MIC. Peptide-PNA sequences are listed in Table 1. Synthesis of *NlpE,* BaeR, and RcsB proteins were induced with 0.1 mM IPTG, whereas PspF and RpoE synthesis were induced with 0.01 mM IPTG.

is a major part of the elevated tolerance to antimicrobials delivered by arginine-rich CPPs in Evo-3 but that additional mutations are required to reach RXR-PNA resistance. As observed for *waaBO*, *gltF*, and *yhcA*, not all mutations from the ALE experiment on their own resulted in low-level resistance to PNA delivered by arginine-rich CPPs. Either these mutations require another mutation to synergistically enable low-level resistance to RXR-PNA or they were selected as mutations that compensate the fitness cost observed in Evo-1 to 3. Indeed, strains with the highest MIC observed to RXR-PNA have increased doubling time, highlighting that this comes with a cost.

The *cpx** phenotype relies on a functional Cpx-system

We show that alterations in the first transmembrane domain of CpxA can produce a *cpx** phenotype. Several gain-of-function mutations in *cpxA* have been reported,[19,20] but most cluster to and around the second transmembrane domain of CpxA.[20] We suggest that the two-amino acid deletion in the first transmembrane domain leads to a conformational change in the periplasmic part of CpxA, which either disallows CpxP regulation or simulates the stress signal that actives the Cpx response, i.e., a constitutive active CpxA. To the best of our knowledge, *cpxR*$_{L20Q}$ is the first reported mutation in *cpxR* resulting in a *cpx** phenotype. The activated Cpx response in the *cpxR*$_{L20Q}$ mutant was CpxA dependent; i.e., the *cpxR*$_{L20Q}$ mutation does not result in a constitutive phosphorylated CpxR. Therefore, it is likely that the *cpxR*$_{L20Q}$ mutation inhibits/diminishes the ability of CpxA to dephosphorylate CpxR-P to CpxR, which in turn results in a constitutive active Cpx response. CpxA and CpxR-P both function as dimers.[41] Thus overproducing the respective wild-type allele in the two mutants restored sensitivity to RXR-PNA by either hetero-dimerization of a mutated and a wild-type protein, with the wild type being dominant to the mutant, or by homo-dimerization of either mutated or wild-type proteins but with wild-type dimer domination due to abundance.

The cytoplasmic membrane is the main barrier for arginine-rich CPP translocation

Loss of *waaB* and *waaO* did not alter susceptibility to PNA or APIM delivered by arginine-rich CPPs, but it increased sensitivity to two cationic AMPs (Table 3). Thus, the uptake of RXR-PNA and R11-APIM is not influenced by the outer core of LPS. A reduction of $\Delta\Psi$ in the cytoplasmic membrane decreased sensitivity to RXR-PNA, R11-APIM, and aminoglycosides. This strongly indicates that the resistance mechanism relies on restricted uptake of the antimicrobials across the cytoplasmic membrane. The magnitude of $\Delta\Psi$ was

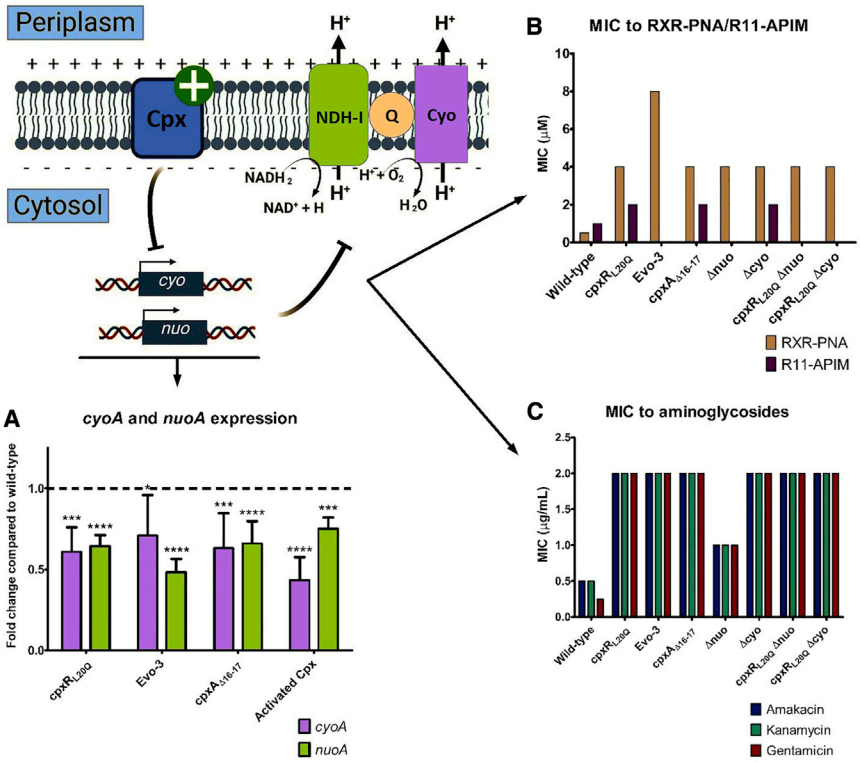

Figure 3. Cpx-mediated downregulation of NDH-I and cytochrome bo_3 oxidase leads elevated tolerance to R11-APIM, RXR-PNA, and aminoglycosides

A schematic model of an activated Cpx response (shown here with a green plus sign) that leads to downregulation of both *nuoA* (NDH-I) and *cyoA* (cytochrome bo_3 oxidase), which consequently results in increased tolerance to RXR-PNA/R11-APIM and aminoglycosides. (A) *nuoA* and *cyoA* expression determined by qRT-PCR(see Materials and methods). All values are indicated as fold change relative to wild type (dashed line). Experiments were performed in biological triplicates. Significant differences are identified (*$p < 0.05$, ***$p < 0.001$, ****$p < 0.0001$) as determined by Bonferroni's multiple-comparison post-test. (B and C) MIC values for RXR-PNA/R11-APIM (in μM) and aminoglycosides (kanamycin, amikacin, and gentamicin in μg/mL) for wild type and mutants. MICs were determined with broth dilutions (see Materials and methods) at 37°C (no shaking). Peptide-PNA sequences are listed in Table 1.

previously found to determine aminoglycoside uptake across the cytoplasmic membrane in *Bacillus subtilis* and *E. coli*[42] but has never been reported for arginine-rich CPP translocation in bacteria. In wild-type cells, RXR-PNA (and possibly also aminoglycosides and R11-APIM) does not significantly activate the Cpx response. When delivered to the inside of the bacterial cell, the antimicrobial part arrests growth; aminoglycosides by interacting with the 30S subunit of ribosomes, PNA by preventing *acpP* translation, and APIM by preventing β-clamp function (Figure 5A). We propose that *cpx**-dependent low-level resistance to RXR-PNA, R11-APIM, and aminoglycosides relies on a decreased $\Delta\Psi$ component of the PMF, resulting from downregulation of respiratory complexes in the cytoplasmic membrane (Figure 5B). Thus, transport of these across the cytoplasmic membrane is expected to become less favorable because of either lack of active cotransport dependent on $\Delta\Psi$ and/or a thermodynamically less favorable diffusion. The more detailed mechanism of membrane passage is not known but could rely on direct penetration or be aided by one or more still-unidentified transporter protein(s). However, data presented neither here nor previously[7] provides evidence for the existence of a singular RXR transport mechanism, but we cannot exclude that RXR is the substrate of multiple transport systems, in which case the absence of one would be compensated by the remaining other(s). Here, Evo-1 to 3 remained sensitive to PNA delivered by the lysine-phenylalanine-rich CPP, KFF, and other cationic peptides. Therefore, these are internalized in a manner independent of the magnitude of the $\Delta\Psi$, like the SbmA-dependent uptake mechanisms for KFF-PNA.[7]

Overall, our data show that the cytoplasmic membrane is the main barrier for uptake of arginine-rich peptides and that crossing is dependent on the electric potential across the membrane. Consequently, uptake can be restricted by activation of Cpx envelope stress response due to downregulation of respiratory operons resulting in a reduction in the electric potential. The latter also explains cross-resistance between antimicrobials delivered by arginine-rich peptides and aminoglycosides. Two newly identified Cpx mutations give further insight into sensing and activation of the Cpx system.

MATERIALS AND METHODS

Additional materials and methods are found in Supplemental materials and methods.

Growth conditions

All strains are listed in Table S4. Cells were grown in Luria-Bertani Broth (LB) medium or Müller-Hinton I Broth (MHBI) at 37°C with aeration unless stated otherwise. When necessary, antibiotics were added to the following concentrations: chloramphenicol, 20 μg/mL; ampicillin, 150 μg/mL; kanamycin, 50 μg/mL; tetracycline, 10 μg/mL.

Peptide conjugates

PNA-peptide conjugates were synthesized as described previously.[1,7] R11-APIM (RWLVK* with the complete sequence Ac-MD-RWLVK-GILQWRKI-RRRRRRRRRRR) has been described previously.[21]

Adaptive laboratory evolution experiment

Wild type was evolved for 20 days to CPP_{RXR}-PNA, with two lineages evolved in parallel for each drug. Here, 1×10^5 colony-forming units (CFU)/mL of cells were inoculated in 2-fold peptide-PNA gradient in 8 dilutions in 100 μL of MHBI in a 96-well polystyrene microtiter plate

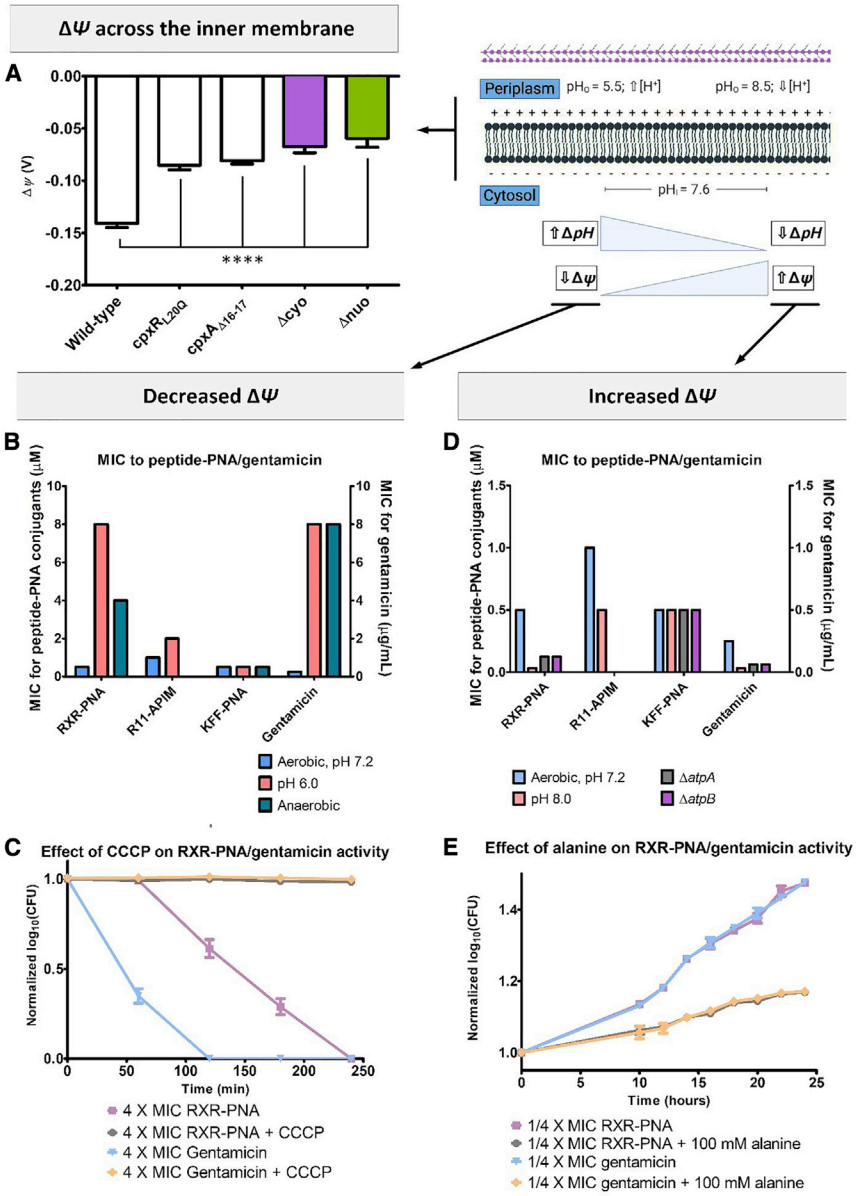

Figure 4. The magnitude of ΔΨ across the cytoplasmic membrane determines RXR-PNA and aminoglycoside tolerance

(A) ΔΨ across the cytoplasmic membrane as measured by the TPP^+ uptake for wild type, $cpxR_{L20Q}$, $cpxA_{\Delta 16\text{-}17}$, Δ*cyo*, and Δ*nuo*. Experiments were performed as a minimum in biological triplicates. Lines under the bar indicate that significant differences were identified (****p < 0.0001) as determined by Bonferroni's multiple-comparison post-test. (B) MIC determinations for wild type tested against RXR-PNA, R11-APIM, KFF-PNA, and gentamicin anaerobically or at pH 6.0. Peptide-PNA/APIM MICs are given in μM (left y axes), and gentamicin MICs are given in μg/mL (right y axes). Wild-type MICs are given for aerobic growth conditions at pH 7.2 identical to the growth conditions for the ALE experiment. (C) Wild-type cells were treated with four times the MIC of RXR-PNA (2 μM) or gentamicin (2 μg/mL) with or without the addition of 50 μM carbonyl cyanide *m*-chlorophenyl hydrazine (CCCP). Samples were collected at time 0 and each following hour up to 4 h after treatment. The $\log_{10}$ CFU counts are normalized to time 0 and plotted over time. The experiments were performed in triplicate. (D) MIC determinations for wild type tested against RXR-PNA, R11-APIM, KFF-PNA, and gentamicin at pH 8.0 or with either of the ATP synthase subunits *atpA* (subunit F1) or *atpB* (subunit F0) deleted. Peptide-PNA MICs are given in μM (left y axes), and gentamicin MICs are given in μg/mL (right y axes). Wild-type MICs are given for aerobic growth conditions at pH 7.2 identical to the growth conditions for the ALE experiment. (E) Wild-type cells grown in minimal media containing acetate were treated with a quarter of the MIC of RXR-PNA (0.125 μM) or gentamicin (0.125 μg/mL) with or without the addition of 100 mM alanine. Samples were collected at time 0 and each following hour up to 24 h after treatment. The $\log_{10}$ CFU counts are normalized to time 0 and plotted over time. The experiments were performed in triplicate.

and grown for 18–24 h at 37°C. The following day, the population grown in the highest concentration of peptide-PNA were re-diluted to 1×10^5 CFU/mL and inoculated in a fresh 2-fold peptide-PNA gradient as above. After 20 successive passages, five peptide-PNA-resistant single clones were isolated from each lineage and whole genome sequenced. As control, *E. coli* MG1655 was evolved to the MHBI in four independent biological replicates without the presence of peptide-PNA. Here, two clones were isolated and whole genome sequenced for each lineage.

Whole genome sequencing and data analysis

Reads were mapped to MG1655 NC_000913.3 with BWA-MEM. Variants were extracted with Freebayes (only variants with >50% frequency were retained). For location of IS insertion, mapped reads with <60 mapQuality were selected and paired reads (CIGAR-Left-clip/Right-Clip, CIGAR-D and CIGAR-I) were aligned to NC_000913.3 by using NCBI Blast to confirm deletion/insertion.

Antimicrobial susceptibility testing

MIC values were determined by broth microdilution according to the standard protocol[43] with a few modifications. Briefly, an overnight bacterial cell culture was diluted to ~5×10^5 CFU/mL in MHBI. 100 μL of bacterial solution was dispensed into a low-bind 96-well plate (Thermo Scientific, cat.no. 260895) along with 11 μL of the test compound (2-fold dilutions). The plate was incubated at 37°C for 18–24 h. The MIC was determined as the lowest concentration that inhibited visible growth in the wells (OD_{595} nm < 0.1). Peptide-PNAs were dissolved in 0.02% acetic acid containing 0.4% bovine serum albumin (BSA), and dilutions were performed in 0.01% acetic acid containing 0.2% BSA, while gentamicin, amikacin, kanamycin, cecropin P1, Cap11 (GenScript), Cap18 (GenScript), apidaecin 1B (GenScript), colistin, indolicidin, and protamine (Sigma-Aldrich) were diluted according to vendors' specifications. To determine MICs under acidic and alkaline conditions, MHBI was

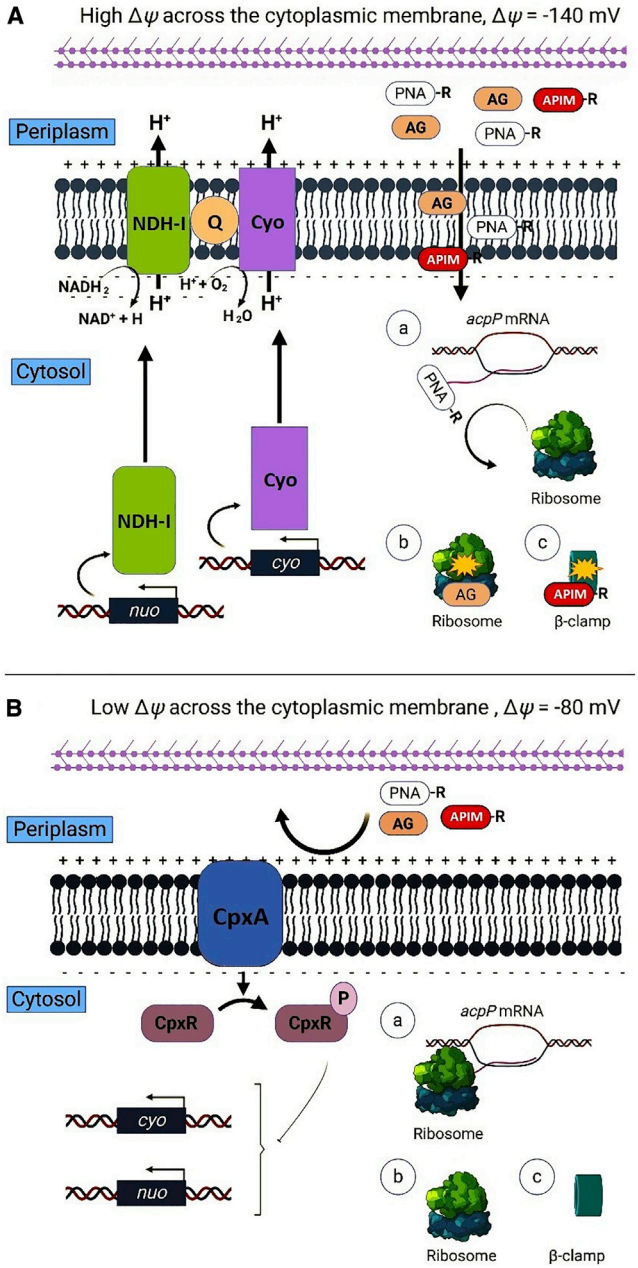

Figure 5. RXR-PNA, R11-APIM, and aminoglycoside uptake in wild-type and *cpx cells**

A schematic model of RXR-PNA, R11-APIM, and aminoglycoside (AG) internalization across the cytoplasmic membrane and action in wild type (A) and a *cpx** mutant (B). (A) In the wild type, RXR-PNA, R11-APIM, and aminoglycoside crossing of the cytoplasmic membrane from the periplasmic space and into the cytosol correlates with the magnitude of the $\Delta\Psi$. The respiratory complexes NADH:ubiquinone oxidoreductase complex I (NDH-I) transcribed from the *nuoABCEFGHIJKLMN*-operon (*nuo*) and cytochrome bo_3 ubiquinol oxidase (Cyo) transcribed from the *cyoABCDE* operon (*cyo*) are shown. RXR-PNA, AG, and R11-APIM in the cytosol lead to growth arrest by steric hindrance of ribosome binding to *acpP* mRNA for RXR-PNA (Aa), binding to the 30S subunit of ribosomes impairing translational accuracy (Ab), and binding to the β-clamp, respectively. (B) In a *cpx** mutant, RXR-PNA, R11-APIM, and AG are not able to transvers the cytoplasmic membrane from the periplasmic space and into the cytosol. The constitutive active Cpx response downregulates *nuo* and *cyo*, which results in a reduced $\Delta\Psi$, which correlates with reducing killing for all the compounds. Lack of RXR-PNA and AG in the cytosol leads to translation of *acpP* mRNA (Ba), wild-type-like 30S ribosomal function (Bb), and wild-type-like β-clamp function, respectively, both leading to survival during RXR-PNA, R11-APIM, and AG treatment.

Table 3. $cpxR_{L20Q}$ and $cpxA_{\Delta 16\text{-}17}$ do not provide tolerance to cationic antimicrobial peptides

Minimum inhibitory concentration to peptide-PNA (in μM) and AMPs (in μg/mL)					
AMP/strain	Wild type	$cpxA_{\Delta 16\text{-}17}$	$cpxR_{L20Q}$	Δ*waaBO*	Evo-3
RXR-PNA	0.5	4	4	0.5	8
Cecropin P1	32	32	32	16	16
Cap11	2	2	2	1	1
Cap18	2	2	2	1	1
Indolicidin	4	4	4	4	4
Apidaecin 1B	8	8	8	8	8
Colistin	0.125	0.125	0.125	0.0625	0.0625
Protamine	16	16	16	16	16

MIC values for peptide-PNA (in μM) and AMPs (in μg/mL) for wild type and indicated mutants. MICs were determined with broth dilutions (see Materials and methods) at 37°C (no shaking). Peptide-PNA sequences are listed in Table 1.

buffered to pH 6.0 or pH 8.0 with citrate buffer (pH 3.0) and carbonate-bicarbonate buffer (pH 10.0), respectively. Anaerobic growth for MIC determinations was performed in a double-sealed bag, using anaerobic atmosphere generation bags (Becton Dickinson, Franklin Lakes, NJ, USA). MHBI was supplemented with 0.1 mM IPTG when tested strains harbored pCA24n-based plasmids, except for pCA24n:*pspF* and pCA24n:*rpoE*, which were induced with 0.01 mM IPTG.

Antibiotic bacteriocidal assay using L-alanine

The effect of alanine on tolerance to RXR-PNA and aminoglycosides was tested as previously described by Peng et al.,[44] with a few modifications. Briefly, overnight cultures were collected by centrifugation at 8.000 rpm for 5 minutes, washed twice in 0.9% NaCl solution, and resuspended to an OD_{600} of 0.5 in ABT minimal medium. Samples were then diluted to 5×10^5 CFU/mL in 10 mL of the same medium supplemented with or without 100 mM alanine and RXR-PNA or gentamicin. After 10 h of incubation at 37°C, a 100 μL aliquot was periodically removed, serially diluted in 0.9% NaCl, spotted onto LB agar plates, and incubated at 37°C overnight, and CFU were calculated. The data were normalized by dividing the CFU obtained from a treated sample by the CFU obtained from the control sample. The study was performed in a biological triplicate.

Antibiotic bacteriocidal assay using carbonyl cyanide *m*-chlorophenyl hydrazone

Time-kill curves were performed for RXR-PNA and gentamicin, as previously described,[45] with minor modifications. Shortly, overnight

cultures were diluted to 5×10^5 CFU/mL in MHBI. Samples were pretreated with 50 μM CCCP for 5 min. CCCP was dissolved in dimethyl sulfoxide (DMSO), and the same amount of DMSO was added to the control sample. After CCCP treatment RXR-PNA or gentamicin was added at 4× MIC concentration (time zero). A 100 μL aliquot was periodically removed, serially diluted down to 1,000-fold in 0.9% NaCl, and spotted onto LB agar plates, followed by incubation at 37°C overnight, and CFU/mL was determined. The study was performed in a biological triplicate.

qRT-PCR

For qRT-PCR experiments, after genomic DNA digestion, 1 μg of total RNA was retrotranscribed with the QuantiTect Reverse Transcription Kit (QIAGEN). Primers designed to amplify *cpxP*, *nuoA*, and *cyoA* (Table S5) were targeted to regions of unique sequences within the genes in wild-type *E. coli* MG1655. The qRT-PCR was performed with TB Green Premix Ex Taq II (Takara Bio, Shiga, Japan) on a QuantStudio 3 Real-Time PCR System (Thermo Fisher Scientific, Waltham, MA, USA). All data were normalized to the reference genes *hctA* and *cysG*. These data were transformed to log2 to obtain a change difference (n-fold) between strains.

Determination of ΔΨ by measuring TPP^+ uptake with the TPP^+-selective electrode method

The ΔΨ was determined by measuring the uptake of the permeating lipophilic cationic probe TPP^+ (Merck, Germany). An overnight culture was diluted (5.000-fold) in MHBI, and cells from 25 mL of culture were harvested when OD_{595} reached 0.2. Cells were washed twice in 0.1 M Tris·HCl (pH 8.1) under the conditions mentioned above, and the pellets were gently resuspended in 1 mL of the same buffer. To generate cells permeable to TPP^+, after a first incubation for 6 min at 36°C with occasional agitation, bacteria were treated with K^+-EDTA to a concentration of 10 mM and then incubated at 36°C for 3 more minutes. Cells were diluted 10-fold in ice-cold 0.1 M potassium phosphate buffer (0.1 M K_2HPO_4, 0.1 M KH_2PO_4; pH 7.5), to remove EDTA, followed by immediate centrifugation in the cold at 13.000 rpm for 7 min. The cells were washed twice in the same ice-cold buffer with the parameters mentioned above, and the pellets were resuspended to an OD_{595} of 20.0 in 10 mM potassium phosphate buffer (pH 7.5) containing 200 mM NaCl, 0.14 mM $CaCl_2$, 0.1 mM $MgSO_4$, and 0.01 mM $MnCl_2$. The cells were kept on ice until use.

Bacteria were added to an OD_{595} of 4.0 in 10 mL of the same buffer supplemented with glucose and TPP^+ to a concentration of 5 mM and 10 μM, respectively, and TPP^+ uptake was measured with the TPP^+-selective electrode method described by Hosoi et al.[46] TPP^+ concentration in the external medium was determined with a Kwik-Tip Ag/AgCl half-cell electrode, which was constructed according to the instructions provided by the manufacturer (World Precision Instruments, Sarasota, FL, USA). Both the TPP^+-selective electrode and a Flexible Dri-Ref reference electrode (World Precision Instruments, Sarasota, FL, USA) were connected to a Jenway 3510 ion meter (Cole-Parmer, Staffordshire, UK) and the LabTrax 4-Channel Data Acquisition system (WPI). Finally, TPP^+ uptake measurements were carried out in a 15 mL closed tube at 30°C and pH 7.5 for 10 min, and data were recorded with iWorx LabScribe recording and analysis software (iWorx Systems, Dover, NH, USA).

Statistical analysis

Statistical analyses for all experiments were performed with GraphPad Prism 9.0 (GraphPad Software, San Diego, CA, USA; www.graphpad.com). Data from three independent replicates of all groups and controls were compared with one- or two-way analysis of variance (ANOVA) followed by Bonferroni's multiple-comparison post-test. Between groups compared, differences were considered significant at a p value of <0.05.

Data and material availability

All data needed to evaluate the conclusions in the paper are present in the paper and/or the Supplemental information. Additional data are available from authors upon request.

SUPPLEMENTAL INFORMATION

Supplemental information can be found online at https://doi.org/10.1016/j.omtn.2021.06.009.

ACKNOWLEDGMENTS

This paper is dedicated to the memory of Mads Christian Guldbæk (1991–2019). This research was funded by grants from the Danish National Research Foundation (DNRF120), the Novo Challenge Center for Peptide-Based Antibiotics (NNF16OC0021700), A.P. Møller Lægefonden, Augustinus Fonden, Aase og Ejnar Danielsens Fond, Brødrene Hartmanns Fond, the program NTNU Health at Norwegian University of Science and Technology (NTNU), and the Trond Mohn foundation, Norway. We are grateful for the acquisition of strains TR530, MC3, GEB658, and CAG16037 from Philippe Bouloc. All figures were created with BioRender.com.

AUTHOR CONTRIBUTIONS

Conceptualization: J.F.-M., P.E.N, and A.L.-O.; data curation: J.F.-M. and A.K.; formal analysis: J.F.-M., A.K., and A.L.-O.; investigation: J.F.-M. and A.K.; methodology: J.F.-M., A.K., G.C., and A.L.-O.; project administration: J.F.-M. and A.L.-O.; resources: J.F.-M., P.E.N., and A.L.-O.; bioinformatics: G.C.; supervision: P.E.N and A.L.-O.; manuscript writing: J.F.-M.; manuscript editing: J.F.-M., A.K., G.C., M.O., P.E.N., and A.L.-O.

DECLARATION OF INTERESTS

The authors declare no competing interests.

REFERENCES

1. Good, L., and Nielsen, P.E. (1998). Antisense inhibition of gene expression in bacteria by PNA targeted to mRNA. Nat. Biotechnol. *16*, 355–358.

2. Wesolowski, D., Tae, H.S., Gandotra, N., Llopis, P., Shen, N., and Altman, S. (2011). Basic peptide-morpholino oligomer conjugate that is very effective in killing bacteria by gene-specific and nonspecific modes. Proc. Natl. Acad. Sci. USA *108*, 16582–16587.

3. Good, L., Sandberg, R., Larsson, O., Nielsen, P.E., and Wahlestedt, C. (2000). Antisense PNA effects in Escherichia coli are limited by the outer-membrane LPS layer. Microbiology (Reading) *146*, 2665–2670.
4. Mitchell, D.J., Kim, D.T., Steinman, L., Fathman, C.G., and Rothbard, J.B. (2000). Polyarginine enters cells more efficiently than other polycationic homopolymers. J. Pept. Res. *56*, 318–325.
5. Futaki, S., and Nakase, I. (2017). Cell-Surface Interactions on Arginine-Rich Cell-Penetrating Peptides Allow for Multiplex Modes of Internalization. Acc. Chem. Res. *50*, 2449–2456.
6. Habault, J., and Poyet, J.L. (2019). Recent Advances in Cell Penetrating Peptide-Based Anticancer Therapies. Molecules *24*, 927.
7. Ghosal, A., Vitali, A., Stach, J.E., and Nielsen, P.E. (2013). Role of SbmA in the uptake of peptide nucleic acid (PNA)-peptide conjugates in E. coli. ACS Chem. Biol. *8*, 360–367.
8. Munita, J.M., and Arias, C.A. (2016). Mechanisms of Antibiotic Resistance. Microbiol. Spectr. *4*, 10.1128/microbiolspec.VMBF-0016-2015.
9. Ingledew, W.J., and Poole, R.K. (1984). The respiratory chains of Escherichia coli. Microbiol. Rev. *48*, 222–271.
10. Kashket, E.R. (1985). The proton motive force in bacteria: a critical assessment of methods. Annu. Rev. Microbiol. *39*, 219–242.
11. Vik, S.B., and Antonio, B.J. (1994). A mechanism of proton translocation by F1F0 ATP synthases suggested by double mutants of the a subunit. J. Biol. Chem. *269*, 30364–30369.
12. Gunner, M.R., Amin, M., Zhu, X., and Lu, J. (2013). Molecular mechanisms for generating transmembrane proton gradients. Biochim. Biophys. Acta *1827*, 892–913.
13. Bury-Moné, S., Nomane, Y., Reymond, N., Barbet, R., Jacquet, E., Imbeaud, S., Jacq, A., and Bouloc, P. (2009). Global analysis of extracytoplasmic stress signaling in Escherichia coli. PLoS Genet. *5*, e1000651.
14. Raivio, T.L., Leblanc, S.K., and Price, N.L. (2013). The Escherichia coli Cpx envelope stress response regulates genes of diverse function that impact antibiotic resistance and membrane integrity. J. Bacteriol. *195*, 2755–2767.
15. Weber, R.F., and Silverman, P.M. (1988). The cpx proteins of Escherichia coli K12. Structure of the cpxA polypeptide as an inner membrane component. J. Mol. Biol. *203*, 467–478.
16. Itou, H., and Tanaka, I. (2001). The OmpR-family of proteins: insight into the tertiary structure and functions of two-component regulator proteins. J. Biochem. *129*, 343–350.
17. Raivio, T.L., Popkin, D.L., and Silhavy, T.J. (1999). The Cpx envelope stress response is controlled by amplification and feedback inhibition. J. Bacteriol. *181*, 5263–5272.
18. Buelow, D.R., and Raivio, T.L. (2005). Cpx signal transduction is influenced by a conserved N-terminal domain in the novel inhibitor CpxP and the periplasmic protease DegP. J. Bacteriol. *187*, 6622–6630.
19. Danese, P.N., Snyder, W.B., Cosma, C.L., Davis, L.J., and Silhavy, T.J. (1995). The Cpx two-component signal transduction pathway of Escherichia coli regulates transcription of the gene specifying the stress-inducible periplasmic protease, DegP. Genes Dev. *9*, 387–398.
20. Raivio, T.L., and Silhavy, T.J. (1997). Transduction of envelope stress in Escherichia coli by the Cpx two-component system. J. Bacteriol. *179*, 7724–7733.
21. Nedal, A., Ræder, S.B., Dalhus, B., Helgesen, E., Forstrøm, R.J., Lindland, K., Sumabe, B.K., Martinsen, J.H., Kragelund, B.B., Skarstad, K., et al. (2020). Peptides containing the PCNA interacting motif APIM bind to the β-clamp and inhibit bacterial growth and mutagenesis. Nucleic Acids Res. *48*, 5540–5554.
22. Liu, X., Li, Y., Guo, Y., Zeng, Z., Li, B., Wood, T.K., Cai, X., and Wang, X. (2015). Physiological Function of Rac Prophage During Biofilm Formation and Regulation of Rac Excision in Escherichia coli K-12. Sci. Rep. *5*, 16074.
23. Castaño, I., Bastarrachea, F., and Covarrubias, A.A. (1988). gltBDF operon of Escherichia coli. J. Bacteriol. *170*, 821–827.
24. Raetz, C.R., and Dowhan, W. (1990). Biosynthesis and function of phospholipids in Escherichia coli. J. Biol. Chem. *265*, 1235–1238.
25. Alksne, L.E., Anthony, R.A., Liebman, S.W., and Warner, J.R. (1993). An accuracy center in the ribosome conserved over 2 billion years. Proc. Natl. Acad. Sci. USA *90*, 9538–9541.
26. Ebbensgaard, A., Mordhorst, H., Aarestrup, F.M., and Hansen, E.B. (2018). The Role of Outer Membrane Proteins and Lipopolysaccharides for the Sensitivity of *Escherichia coli* to Antimicrobial Peptides. Front. Microbiol. *9*, 2153.
27. Otto, K., and Silhavy, T.J. (2002). Surface sensing and adhesion of Escherichia coli controlled by the Cpx-signaling pathway. Proc. Natl. Acad. Sci. USA *99*, 2287–2292.
28. Price, N.L., and Raivio, T.L. (2009). Characterization of the Cpx regulon in Escherichia coli strain MC4100. J. Bacteriol. *191*, 1798–1815.
29. Nitta, T., Nagamitsu, H., Murata, M., Izu, H., and Yamada, M. (2000). Function of the sigma(E) regulon in dead-cell lysis in stationary-phase Escherichia coli. J. Bacteriol. *182*, 5231–5237.
30. Hirota, N., Matsuura, S., Mochizuki, N., Mutoh, N., and Imae, Y. (1981). Use of lipophilic cation-permeable mutants for measurement of transmembrane electrical potential in metabolizing cells of Escherichia coli. J. Bacteriol. *148*, 399–405.
31. Suzuki, T., Murakami, T., Iino, R., Suzuki, J., Ono, S., Shirakihara, Y., and Yoshida, M. (2003). F0F1-ATPase/synthase is geared to the synthesis mode by conformational rearrangement of epsilon subunit in response to proton motive force and ADP/ATP balance. J. Biol. Chem. *278*, 46840–46846.
32. Kasianowicz, J., Benz, R., and McLaughlin, S. (1984). The kinetic mechanism by which CCCP (carbonyl cyanide m-chlorophenylhydrazone) transports protons across membranes. J. Membr. Biol. *82*, 179–190.
33. Jensen, P.R., and Michelsen, O. (1992). Carbon and energy metabolism of atp mutants of Escherichia coli. J. Bacteriol. *174*, 7635–7641.
34. Ye, J.Z., Su, Y.B., Lin, X.M., Lai, S.S., Li, W.X., Ali, F., Zheng, J., and Peng, B. (2018). Alanine Enhances Aminoglycosides-Induced ROS Production as Revealed by Proteomic Analysis. Front. Microbiol. *9*, 29.
35. Evans, M.E., Feola, D.J., and Rapp, R.P. (1999). Polymyxin B sulfate and colistin: old antibiotics for emerging multiresistant gram-negative bacteria. Ann. Pharmacother. *33*, 960–967.
36. Gutsmann, T., Fix, M., Larrick, J.W., and Wiese, A. (2000). Mechanisms of action of rabbit CAP18 on monolayers and liposomes made from endotoxins or phospholipids. J. Membr. Biol. *176*, 223–236.
37. Johansen, C., Verheul, A., Gram, L., Gill, T., and Abee, T. (1997). Protamine-induced permeabilization of cell envelopes of gram-positive and gram-negative bacteria. Appl. Environ. Microbiol. *63*, 1155–1159.
38. Gazit, E., Boman, A., Boman, H.G., and Shai, Y. (1995). Interaction of the mammalian antibacterial peptide cecropin P1 with phospholipid vesicles. Biochemistry *34*, 11479–11488.
39. Subbalakshmi, C., and Sitaram, N. (1998). Mechanism of antimicrobial action of indolicidin. FEMS Microbiol. Lett. *160*, 91–96.
40. Florin, T., Maracci, C., Graf, M., Karki, P., Klepacki, D., Berninghausen, O., Beckmann, R., Vázquez-Laslop, N., Wilson, D.N., Rodnina, M.V., and Mankin, A.S. (2017). An antimicrobial peptide that inhibits translation by trapping release factors on the ribosome. Nat. Struct. Mol. Biol. *24*, 752–757.
41. Mechaly, A.E., Haouz, A., Sassoon, N., Buschiazzo, A., Betton, J.M., and Alzari, P.M. (2018). Conformational plasticity of the response regulator CpxR, a key player in Gammaproteobacteria virulence and drug-resistance. J. Struct. Biol. *204*, 165–171.
42. Bryan, L.E., and Kwan, S. (1983). Roles of ribosomal binding, membrane potential, and electron transport in bacterial uptake of streptomycin and gentamicin. Antimicrob. Agents Chemother. *23*, 835–845.
43. Hancock, R.E.W. (1999). MIC Determination By Microtitre Broth Dilution Method, http://cmdr.ubc.ca/bobh/method/mic-determination-by-microtitre-broth-dilution-method/.
44. Peng, B., Su, Y.B., Li, H., Han, Y., Guo, C., Tian, Y.M., and Peng, X.X. (2015). Exogenous alanine and/or glucose plus kanamycin kills antibiotic-resistant bacteria. Cell Metab. *21*, 249–262.
45. Goltermann, L., and Nielsen, P.E. (2020). PNA Antisense Targeting in Bacteria: Determination of Antibacterial Activity (MIC) of PNA-Peptide Conjugates. In Peptide Nucleic Acids: Methods and Protocols, P.E. Nielsen, ed. (New York, NY: Springer US), pp. 231–239.
46. Hosoi, S., Mochizuki, N., Hayashi, S., and Kasai, M. (1980). Control of membrane potential by external H+ concentration in Bacillus subtilis as determined by an ion-selective electrode. Biochim. Biophys. Acta *600*, 844–852.